Journal of Power Sources, *32* (1990) 125 - 133

CHARACTERIZATION OF NICKEL OXIDE IN MOLTEN CARBONATE I. ELECTROCHEMICAL BEHAVIOUR OF HIGHER NICKEL OXIDE IN MOLTEN CARBONATE

GANG XIE, YOSHIHARU SAKAMURA, KEIKO EMA and YASUHIKO ITO*

Department of Nuclear Engineering, Faculty of Engineering, Kyoto University, Sakyo-ku, Kyoto 606 (Japan)

(Received December 4, 1989)

Summary

The anodic oxidation of nickel is studied employing several methods, namely, voltammetry, chronopotentiometry, ESCA and X-ray diffraction. The results indicate that two reactions are involved in the anodic process: one is $Ni + O^{2-} = NiO + 2e^-$; the other reaction is considered to be the formation of unstable higher nickel oxide, and perhaps $Ni(II) = Ni(III) + e^-$. The stability of this kind of higher nickel oxide depends, to a great extent, on the ambient partial pressure of oxygen.

Introduction

Molten salts are stable at very high temperature; they are also good conductors of heat and satisfactory solvents. Thus, molten salts have been widely used for producing and refining metals since the early years of this century. Recently, alternative applications of molten salts (such as molten carbonate) have been developed, or suggested, for fuel cells, thermal energy storage, nuclear waste processing, coal gasification, etc. [1, 2].

The molten carbonate fuel cell (MCFC) is believed to be a promising new energy source. MCFC technology offers the possibility for clean and efficient generation of electricity from hydrocarbon fuels and coal. Carbonates are attractive electrolytes because of their compatibility with carbonaceous fuels and because of their operating temperature range, which provides 'waste heat' at a useful temperature of around 650 °C. Nevertheless, there still are many technical problems to be overcome with MCFC systems. For example, carbonate electrolyte is very corrosive and the operating temperature is around 650 °C and, therefore, the stability of the electrode materials as well as construction materials is of prime importance. At present, nickel oxide (lithiated NiO) is used as the positive electrode material

*Author to whom correspondence should be addressed.

0378-7753/90/$3.50

in MCFC systems, but its dissolution presents a major hindrance to MCFC development [3 - 6]. To improve the long-term operating characteristics of a MCFC, it is imperative to obtain a more thorough understanding of the electrochemical behaviour of the electrode. In this paper, an investigation is made of the reaction mechanism of the anodic oxidation of nickel in a molten Li_2CO_3–K_2CO_3 system at 650 °C.

Experimental

The experimental apparatus consisted of a stainless-steel container with a gas-tight stainless-steel cap. Inside the former was placed a high-density alumina crucible of ~500 ml capacity. This crucible contained the electrolyte as well as the working, counter and reference electrodes, together with a gas bubbler tube of pure alumina. The whole unit was heated by means of vertical electric furnace. The Li_2CO_3 and K_2CO_3 powder for the electrolyte were guaranteed grade chemicals (Wako Chemical Co., Ltd). For each run, approximately 500 g of a mixture of Li_2CO_3 and K_2CO_3 in eutectic proportions (Li:K = 62:38) were weighed and placed in the alumina crucible. The eutectic mixture was vacuum dried for at least 48 h at 300 °C and then melted at 650 °C under pure CO_2 gas atmosphere in the apparatus. The latter was pumped down to the CO_2 decomposition pressure for degassing and removal of water vapour. The melt was then saturated with CO_2 by bubbling, to neutralize any O^{2-} formed and to decompose any OH^- present. For each new gas composition, such saturation of the melt by the gas atmosphere was normally conducted overnight.

A nickel disc of 7.0 mm diameter and 3.0 mm thickness was used as the working electrode. The reference electrode employed was the so-called standard oxygen electrode, which consists of coiled gold wire dipping into electrolyte and blanketed with a P_{O_2}/P_{CO_2} = 0.33/0.67 gas mixture. This reference electrolyte was contained in an alumina tube and connected with that in the crucible by way of the liquid carbonate film. The tube had a tiny hole of diameter less than 1.0 mm drilled in it, and was pressed against the flat bottom of the crucible to avoid bubbling of the reference gas mixture from the reference electrode into the main crucible. All values of potential are quoted with respect to the oxygen electrode unless otherwise stated. A gold electrode was used as the counter electrode.

Electrochemical measurements were made with an X-Y recorder (model 3025, Yokogawa Ltd.), a function generator (model HB-105, Hokuto Denko Ltd.) and a potentio/galvanostat (model HA-301, Hokuto Denko Ltd.) interfacing with a 16-bit personal computer, PC9801VX21 (Nippon Electric Co. Ltd.). All the data were processed by this computer.

Results and discussion

A typical voltammogram for the nickel electrode is shown in Fig. 1. The total gas pressure is 1 atm., of which the CO_2 mole fraction is 0.01.

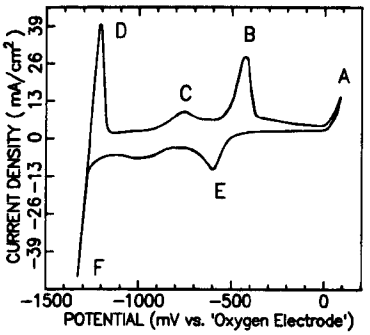

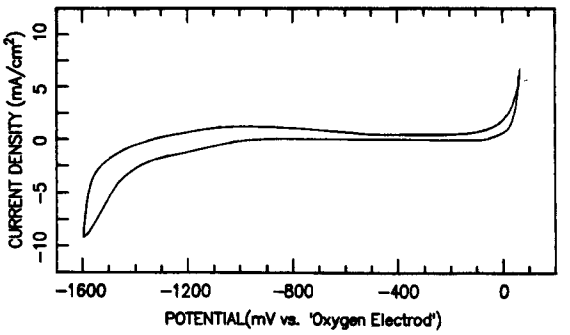

Fig. 1. Voltammogram for nickel electrode measured under P_{Ar}/P_{CO_2} = 0.99/0.01 atm. at 650 °C; scan rate = 50 mV s^{-1}.

Fig. 2. Voltammogram for gold electrode measured under P_{Ar}/P_{CO_2} = 0.99/0.01 atm. at 650 °C; scan rate = 50 mV s^{-1}.

The peak A represents the anodic oxidation of carbonate ion under evolution of carbon dioxide and oxygen. The peak F which commences at around −1200 mV is the cathodic breakdown of the electrolyte. On reversal of the potential sweep, oxidation of the carbon deposit gives rise to peak D. Given that the rest potential of the nickel electrode usually has a value of around −800 to −600 mV, the peak C at about −700 mV represents the formation of normal nickel oxide, NiO. The peak B at −440 mV is the one of special interest in this study. It will be seen later that the only rational explanation for the presence of this peak is the further oxidation of NiO(II) to some kind of higher nickel oxide.

To confirm that the peaks B and C in the voltammogram of Fig. 1 are indeed caused by the oxidation of the nickel electrode, the voltammogram of a gold electrode was taken under the same atmosphere; the result is shown in Fig. 2. Because of the stability of the gold electrode, no reactions are observed over the potential range from −1400 mV to 0 V. Thus, the current recorded is simply that of the background electrolyte, corresponding to that found in the voltammogram for nickel (Fig. 1).

To further identify the voltammetric features of the nickel electrode, chronopotentiometry was carried out at the nickel electrode as well. The resulting curve is shown in Fig. 3 and is for anodic polarization under the same atmosphere as above and at a current density of 26 mA cm^{-2}. Three plateaux appear at potentials of about −700 mV, −400 mV and 0 V; these are coincident with the anodic waves seen on the voltammogram for nickel (Fig. 1). The plateau at −400 mV appears to indicate the existence of a higher nickel oxide.

X-ray diffraction (XRD) analysis was conducted in order to obtain more information about the suspected higher nickel oxide. A sample for such measurement was prepared by potentiostating at −100 mV for 4 h under the same atmosphere referred to above. The XRD pattern given in Fig. 4, was identical to that for normal NiO. Nevertheless, the voltammetric

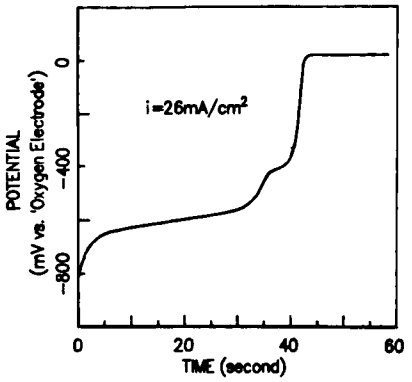

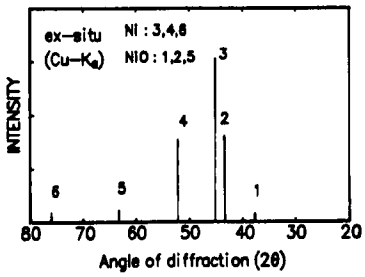

Fig. 3. Chronopotentiogram for nickel electrode measured under P_{Ar}/P_{CO_2} = 0.99/0.01 atm. at 650 °C; current density = 26 mA cm^{-2}.

Fig. 4. XRD pattern for nickel electrode prepared under P_{Ar}/P_{CO_2} = 0.99/0.01 atm. for 4 h at 650 °C.

and the chronopotentiometric results strongly suggest that there must be some kind of higher nickel oxide formed at a potential of −100 mV. To resolve this issue, two possible explanations may be considered: (i) the higher nickel oxide is very unstable, so the film of the oxide is too thin to be detected by XRD analysis; (ii) the crystal lattice of the higher nickel oxide is so similar to that of NiO that the difference of XRD patterns between these two oxides cannot be distinguished.

Chronopotentiometry has a special advantage compared with other electrochemical methods, in that the rate of the electrochemical reaction can be controlled by means of the applied current density. Suppose that the higher nickel oxide of interest exists but is unstable, then if the applied current density is large enough, the electrode reaction, after reaching the second step of the anodic process, *i.e.*, the formation of the higher nickel oxide, will proceed to the next step, *i.e.*, evolution of oxygen at around zero volts. If the applied current density is not so large, however, the electrode reaction will remain at the second step of the anodic process because the rate of decomposition of the higher nickel oxide is faster than that of formation and a complete layer of higher nickel oxide can not be formed due to the instability of the higher nickel oxide.

The above prediction has been verified by chronopotentiometry carried out at the nickel electrode under the same atmosphere, at a current density of 2.6 mA cm^{-2} rather than of 26 mA cm^{-2}. The result is shown in Fig. 5. A low value was deliberately chosen for the electrolysis current density so that even a small change of potential caused by the electrode process could be recorded exactly. Under these conditions, only two plateaux were observed, at potentials of −700 and −440 mV, respectively. The electrode reaction remained at the second plateau, *i.e.*, at the formation reaction of the higher nickel oxide. The plateau potential of about −440 mV (corresponding to the formation of the higher nickel oxide) was unchanged until

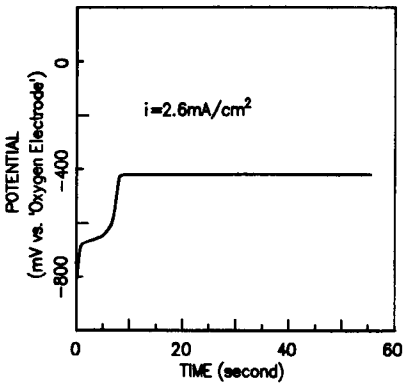

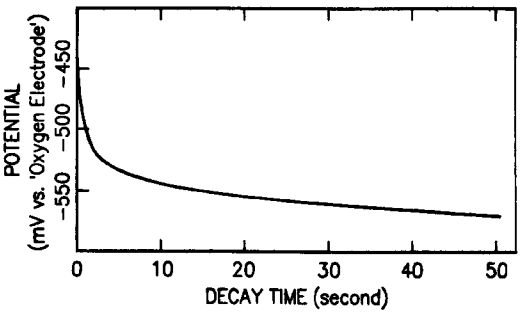

Fig. 5. Chronopotentiogram for nickel electrode measured under P_{Ar}/P_{CO_2} = 0.99/0.01 atm. at 650 °C; current density = 2.6 mA cm^{-2}.

Fig. 6. Potential decay curve for nickel electrode after interruption of anodic polarization current.

the end of the experiment and did not shift to the third potential plateau (corresponding to evolution of oxygen) as was the case in Fig. 3 when the electrolysis current density was large.

After 24 h, the electrolysis current was interrupted, and the potential decay behaviour of the electrode was recorded (Fig. 6). The potential dropped steeply from −440 mV and then approached a steady value corresponding to the rest potential of the nickel electrode. This relaxation pattern confirms the instability of the higher nickel oxide.

The partial pressure of oxygen plays an important role in the decomposition of the oxide. It can be imagined that if the ambient partial pressure of oxygen is sufficiently large, then the higher nickel oxide will be more stable. In such a situation, the electrode reaction can move easily from the second plateau of the anodic process to the third plateau, even at a very small applied current density. This proposition was verified by chronopotentiometric experiments carried out under two kinds of atmosphere, *i.e.*, with and without oxygen, at a very small applied density of 1.3 mA cm^{-2}. The result is shown in Fig. 7.

ESCA was employed in this study to determine the chemical state of electrochemically formed compounds on the electrode surface. Samples for ESCA measurements were prepared under two kinds of atmosphere (namely, P_{Ar}/P_{CO_2} = 0.99/0.01 atm and $P_{Ar}/P_{CO_2}/P_{O_2}$ = 0.25/0.25/0.5 atm) by potentiostating nickel electrodes at potentials of −100 and −500 mV for 24 h, respectively. Usually, the O1s band of NiO has 529.9 eV band energy, and in the presence of Ni_2O_3 the O1s band energy will shift to 531.7 eV [7]. As shown in Fig. 8, for samples prepared at −500 mV under both kinds of atmosphere, namely, (a) and (c), only one kind of oxide, NiO, was detected. In the samples prepared at −100 mV under both atmospheres, namely, (b) and especially (d), two kinds of nickel oxide were detected. These two

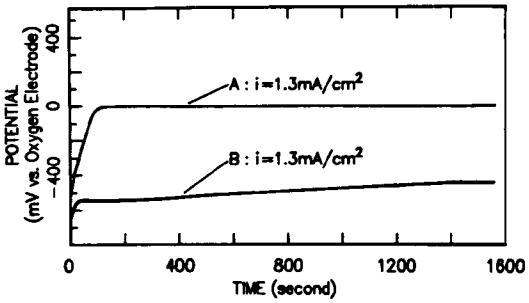

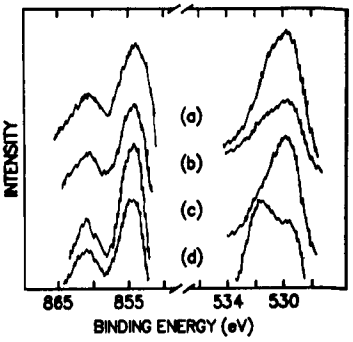

Fig. 7. Chronopotentiogram for nickel electrode measured at 1.3 mA cm^{-2} under: (A) P_{O_2}/P_{CO_2} = 0.99/0.01 atm; (B) P_{Ar}/P_{CO_2} = 0.99/0.01 atm. at 650 °C.

Fig. 8. XPS of $2p_{3/2}$ and O1s levels of nickel samples prepared at 650 °C under P_{Ar}/P_{CO_2} = 0.99/0.01 atm at: (a) −500 mV; (b) −100 mV; and under $P_{Ar}/P_{CO_2}/P_{O_2}$ = 0.25/0.25/0.5 atm at: (c) −500 mV; (d) −100 mV.

oxides are identified as NiO and Ni_2O_3. Under the atmosphere containing oxygen, the peak corresponding to Ni_2O_3 was stronger than that under the atmosphere without oxygen. This is in agreement with the proposed influence of oxygen upon the stability of the higher nickel oxide.

Summarizing the above results and accepting the concept of Ni_2O_3 as a surface defect structure of NiO [7 - 11], the following model is advanced for the reaction mechanism of formation of higher nickel oxide (see Fig. 9). When a nickel ion vacancy is formed on the surface of normal NiO, in order to neutralize the charges carried by the excess oxide ions, the formation of the Ni^{2+} vacancy will be accompanied by the formation of two trivalent nickel ions by oxidation of two bivalent nickel ions adjacent to the vacancy. A thin, monomolecular, trivalent oxide layer is formed and can be considered as a kind of surface defect structure that takes the crystal structure of the substrate, NiO. Generally, the crystal lattice structure of Ni_2O_3 is hexagonal [12], whereas that of NiO is cubic. While the reaction continues, bivalent nickel ions diffuse across the NiO(inner)/Ni_2O_3(outer) interface into the outer phase, and trivalent nickel ions diffuse across the interface into the inner phase. Because of its instability, the trivalent compound will decom-

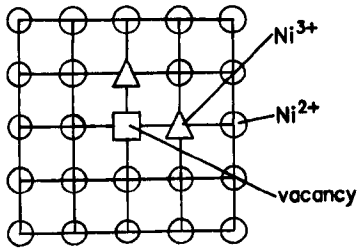

Fig. 9. Schematic of the surface of NiO. The anions are omitted for convenience.

pose into a bivalent one simultaneously. The formation of the vacancy can be expressed as follows:

$$O^{2-}(\text{soln.}) + 2Ni^{2+} = 2Ni^{3+} + 2e^- + [\,] + O^{2-}(\text{lattice}) \quad (1)$$

where: O^{2-}(soln.) and O^{2-}(lattice) represent the oxide in the electrolyte and the oxide in the lattice site, respectively; [ ] is the Ni^{2+} vacancy. The potential of this electrode reaction is given by the Nernst equation:

$$E = E_0 + (RT/2F)\ln[\{(Ni^{3+})^2([\,])(O^{2-})_{\text{lattice}}\}/(Ni^{2+})^2] \quad (2)$$

and the decomposition reaction may be written in the form:

$$Ni^{3+} + \tfrac{1}{2}O^{2-} = Ni^{2+} + \tfrac{1}{4}O_2 \quad (3)$$

If $(Ni^{3+}) = y$, $(Ni^{2+}) = 1 - y - y/2$, $([\,]) = (Ni^{3+})/2 = y/2$ and $(O^{2-})_{\text{lattice}} = 1$, then eqn. (2) becomes:

$$E = E_0 + RT/2F\ln\{y^3/2(1 - y - y/2)^2\} \quad (4)$$

and the rate equation of the decomposition reaction is given by

$$dy/dt = \frac{i}{F} - k_f y + k_b(1 - 3y/2)(P_{O_2})^{0.25} \quad (5)$$

where: i is the electrolysis current density; k_f and k_b are the reaction rate constants of the forward and backward reaction of reaction (3), respectively. For a decay process, namely $i = 0$, the solution of eqn. (5) is:

$$y = \frac{B}{A} + C\exp(-At) \quad (6)$$

where $A = k_f + \frac{3}{2}k_b(P_{O_2})^{0.25}$, $B = k_b(P_{O_2})^{0.25}$ and C is the integral constant. By substituting eqn. (6) into eqn. (4), the E–t relation equation can be written as:

$$E = E_0' + (RT/2F)\ln\left\{\left(\frac{B}{A} + C\exp^{-At}\right)^3 \Big/ \left[1 - 3/2\left(\frac{B}{A} + C\exp^{-At}\right)\right]^2\right\} \quad (7)$$

where: $E_0' = E_0 + (RT/2F)\ln(1/2)$. By suitably choosing the parameters, the E–t plot given by eqn. (7) gives a good approximation to the potential decay curve obtained by experiment. The comparison is shown in Fig. 10.

If either the applied current density or the ambient partial pressure of oxygen is large enough to depress the decomposition, a complete higher nickel oxide layer is formed. So if there exists an optimum environment which is suitable for the growth of Ni_2O_3, a Ni_2O_3 film which possesses its own crystal lattice structure can be formed, and in this situation it can be expected that the characteristic XRD patterns of Ni_2O_3 can be detected, at least *in situ*.

Using the above model, the experimental phenomena can be explained rather satisfactorily. Of course, there is still some uncertainty. For example, some more direct evidence is needed to confirm the existence of Ni_2O_3.

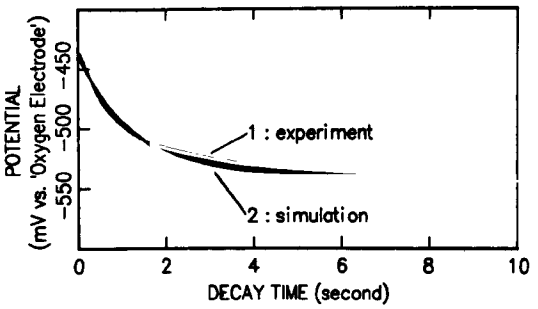

Fig. 10. Comparison between experimental and simulated potential decay curve. (A = 0.09, B = 0.03 and C = 0.15 in eqn. (7)).

Generally, the formation of NiO is accompanied with lithiation. The latter is the dominant factor that determines the conductivity of NiO and allows lithiated NiO to be used as the electrodes in the MCFC system. Naturally, lithiation is expected to exert an influence on the formation of Ni_2O_3. In order to understand more fully the mechanism of the formation of higher nickel oxide, a detailed knowledge of the lithiation process is required.

Because of the instability of the oxide, it is quite difficult to detect it *ex situ*, as is evident from the above 'Results and discussion'. In view of this, a special *in situ* XRD apparatus has been designed in the authors' laboratories. The results obtained with this equipment are reported in a following paper [13].

Conclusions

The anodic oxidation of nickel in molten carbonate has been studied in detail through the use of various investigative techniques. The results reveal that two reactions are involved. One is the formation of bivalent nickel oxide:

$$Ni + O^{2-} = NiO + 2e^- \quad (8)$$

while the other is the further oxidation of bivalent nickel oxide to higher nickel oxide, believed to have the Ni(III) valence:

$$Ni(II) = Ni(III) + e^- \quad (9)$$

This kind of higher nickel oxide is quite unstable, which makes usual *ex situ* surface analysis very difficult. The decomposition of the higher oxide can be represented by the overall reaction:

$$Ni_2O_3 = 2NiO + 1/2O_2 \quad (10)$$

A model has been suggested to elucidate the kinetics of formation and decomposition of the higher nickel oxide.

Acknowledgements

The authors thank Dr M. Matsunaga, Kyusyu Institute of Technology, for his continual interest and helpful comments. Grateful acknowledgment is also made to the Research Center of Fundamental Materials of Sanyo Electric Inc. for support of this work. One author (G.X.) gratefully acknowledges the award of a graduate research scholarship from the People's Republic of China. The work was supported by a Grant-in-Aid from the Japanese Ministry of Education, Science and Culture.

References

1 J. R. Selman and L. G. Marianowski, in D. G. Lovering (ed.), *Molten Salt Technology*, Plenum, New York, 1982, pp. 323 - 393.
2 J. R. Selman and H. C. Maru, in G. Mamantov and J. Braunstein (eds.), *Molten Salt Chemistry*, Vol. 4, Plenum, New York, 1981, pp. 159 - 390.
3 M. L. Orfield and D. A. Shores, *J. Electrochem. Soc., 135* (1988) 1662.
4 J. D. Doyon, T. Gilbert and G. Davies, *J. Electrochem. Soc., 134* (1987) 3035.
5 M. D. Ingram and G. J. Jane, *Electrochim. Acta, 10* (1965) 783.
6 C. E. Baumgartner, *J. Am. Ceram. Soc., 67* (1984) 460.
7 K. S. Kim and N. Winograd, *Surface Sci., 43* (1974) 625.
8 T. Robert, M. Bartel and G. Offergeld, *Surface Sci., 33* (1972) 123.
9 R. Rosencwaig and G. K. Wertheim, *J. Electron Spectrosc. Relat. Phenom., 1* (1972/73) 251.
10 G. Schön, *J. Electron Spectrosc. Relat. Phenom., 1* (1972/73) 105.
11 K. S. Kim and R. E. Davis, *J. Electron Spectrosc. Relat. Phenom., 1* (1972/73) 251.
12 P. S. Aggarwal and A. Goswami, *J. Phys. Chem., 65* (1961) 2105.
13 Gang Xie, Y. Sakamura, K. Ema and Y. Ito, *J. Power Sources, 32* (1990) 135.